CONF-9010212--27

CONF-9010212--27

DE91 005486

CALOR89 Calorimeter Simulations, Benchmarking, and Design Calculations

T. Handler[†], University of Tennessee
J. K. Panakkal and J. Proudfoot
Argonne National Laboratory
L. Cremaldi, B. Moore, and J. J. Reidy
University of Mississippi
R. G. Alsmiller, Jr., P. Fu, and T. A. Gabriel,
Oak Ridge National Laboratory

Paper presented at the
Symposium on Detector Research and Development
for the Superconducting Super Collider
October 15 - 18, 1990
Ft. Worth, Texas

Prepared by the
OAK RIDGE NATIONAL LABORATORY
Oak Ridge, Tennessee 37831
managed by
MARTIN MARIETTA ENERGY SYSTEMS, INC.
for the
U.S. DEPARTMENT OF ENERGY
under contract DE-AC05-84OR21400

[†] Managed by Martin Marietta Energy Systems, Inc. under Contract No. DE-AC05-84OR21400 for the U.S. Department of Energy.

MASTER

DISTRIBUTION OF THIS DOCUMENT IS UNLIMITED

CALOR89 Calorimeter Simulations, Benchmarking, and Design Calclulations

Thomas Handler
University of Tennessee
Job Panakkal and Jim Proudfoot
Argonne National Laboratory
Lucien Cremaldi, Brent Moore, and Jim Reidy
University of Mississippi
Tut Alsmiller, Peter Fu, and Tony Gabriel
Oak Ridge National Laboratory
Presented by Thomas Handler

Symposium on Detector Research and Development
for the Superconducting Super Collider
Ft. Worth, TX Oct 15-18, 1990

Abstract

Results on CALOR89 benchmarking and design calculations utilizing the CALOR89 programs are presented. The benchmarking is done with respect to the ZEUS and D0 calorimeters. The design calculations were done for a variety of absorbers (depleted uranium, lead, and iron) of various thicknesses for a given scintillator thickness and for a fixed absorber thickness using various thicknesses for the scintillator. These studies indicate that a compensating calorimeter can be built using lead as the absorber, whereas a purely iron calorimeter would be non-compensating. A depleted uranium calorimeter would possibly be unsuitable if used in a large configuration and a high luminosity machine because of the delayed energy release from capture gammas.

Introduction

Since the calorimeters that are going to be used at the Superconducting Super Collider (SSC) are going to be large and expensive it would prohibitive to build full scale prototypes. Therefore, the only avenue that is open is to build small scale prototypes that can be tested with the results being compared to the output of simulation programs. These simulation programs can then be used to design the calorimeters, once their accuracy has been established by benchmarking against the existing data. We describe here the CALOR89 simulation code system, the results of benchmarking it with respect to experimental data, and results of design calculations involving various absorber materials and thicknesses and various scintillator thicknesses.

CALOR89

The CALOR89 code system [Fig. 1] consists of four primary programs: HETC88[1], SPECT89, EGS4[2], and MORSE[3] or MICAP[4], plus their ancillary programs and a final analysis program. HETC88 is used to generate and transport the hadronic particles through the calorimeter. HETC88 does the particle transport and generation in a three fold manner: 1) For energies less than 3 GeV particles are generated by means of an

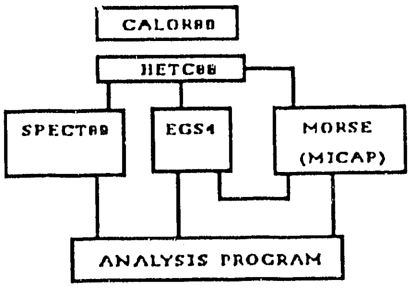

Figure 1. CALOR89 Code System

intermediate-energy Intranuclear-Cascade and Evaporation Model[5]; 2) From 3 GeV to approximately 10 GeV, particle generation is done by means of a scaling model. 3) From 10 Gev upwards particle generation is done by means of FLUKA[6] which uses a multi-chain fragmentation model. Inelastic nucleon hydrogen and charged-pion hydrogen collisions are done via the isobar model or a fragmentation model[1]. The boundary between the use of the Scaling Model and FLUKA is determined by a parameter, ESKALE, that is at the user's discretion. SPECT89 does the energy deposition of the hadrons in the calorimeter. The ancillary program, LIGHT, allows the user to take into account the non-linearity of the light pulse in the scinitllator due to saturation effects within the active medium. This is done by use of Birks' law[7]. In the simulation of calorimeters and the comparison with the experimental test data it is imperative that saturation effects be taken into account. In Figure 2 we show the effects of saturation. The simulation is for a slab calorimeter made from 4mm lead sheet followed by a 1mm sheet of scinitllator repeated to a depth of 150cm. As is seen in the Figure, not taking into account saturation effects, an overestimate is made of the hadronic signal.

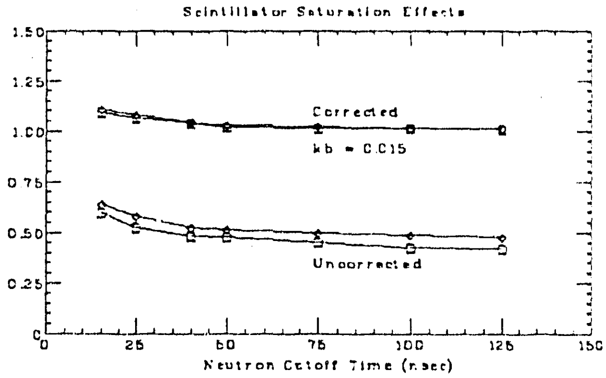

Figure 2. Scintillator Saturation Effects. Lower curves represent uncorrected scinitllator signals, while upper curves have been corrected for saturation effects.

EGS4 is used for the transport and energy deposition of electromagnetic particles in the calorimeter. The source data for EGS4 consists of direct photon production from hadron-nuclear collisions, photons from neutral pion decay, and electrons and positrons from muon decay. These are read from the HETC88 output tape. MORSE or MICAP is used to transport neutrons that are produced with energies less than 20 MeV and to generate the gamma rays from inelastic, fission and capture reactions. These subsequent gammas are then transported by EGS4. Both MORSE and MICAP have time dependence built into the code.

The programs SPECT89, EGS4, and MORSE(MICAP) do **NOT** explicitly incorporate many of the experimental details that are always there. These details include non-uniformity of light collection, electronic noise, pedestal cuts, material noise(natural fission noise), etc. These can be incorporated into the analysis program which combines the output of SPECT89, EGS4, and MORSE(MICAP).

Comparisons of experimental data with CALOR89 calculations should be done with caution. Unless the exact geometries are used, so that leakage out of the sides or the back of the calorimeter is the same, and the exact same materials in the same relative order and the same thicknesses are used, and the value for Birks'constant appropriate for the scintillator is used, the agreement between the simulation results and the experimental data will not be exact.

Benchmarking Results

The results obtained from the CALOR89 code system have been checked against experimental data from the ZEUS prototype lead-scintillator and depleted uranium-scintillator calorimeters, the CDHS iron-scintillator calorimeter and the D0 liquid argon-uranium calorimeter [8-11]. The results of the comparisons are presented in Table I.

TABLE I

CALOR89 Benchmarking Results - e/h

	ZEUS	ZEUS	CDHS	D0
Configuration	DU-SCSN	Pb-SCSN	Fe-SCSN	Liq. Arg.-DU
Thicknesses	0.33/0.26cm	1.00/0.25cm	2.50/0.25cm	0.57/0.3cm
CALOR89	1.01+/-0.03	0.99+/-0.03	1.17+/-0.03	1.06
Experiment	1.01+/-0.04	1.05+/-0.02	.19+/-0.04	1.03+/-.015

As can be seen the overall agreement between the CALOR89 predictions and the experimental data is quite good.

Design Calculations

We have carried out a series of calculations to determine the sensitivity of the compensation and resolution characteristics of a prototypic calorimeter composed of various absorber materials (depleted uranium, lead, and iron) of various thicknesses (0.5, 1.0, 2.0, and 4.0 radiation length) in conjunction with various scintillator thicknesses (0.1, 0.25, 0.5, and 1.0 cm). The incoming particle used was a 10 GeV kinetic energy negative pion and a 10 Gev electron. Birks' constant for the scintillator saturation level was set at 0.0131. The calorimeter was 2m by 2m by 8 interaction lengths of absorber material. The complete matrix of absorber thicknesses and scintillator thicknesses was not explored. In one series of calculations the scintillator thickness was fixed at 0.25cm and the various absorber thicknesses were used. In another series of calculations the absorber thickness was fixed at 1 radiation length and the scintillator thickness was varied. Various gate times were used in the low energy neutron and subsequent gamma analysis. The actual gate time has an uncertainty of approximately 5 - 10 nsec due to the fact that no timing is done in HETC88 or EGS4.

We present in Figure 3 the compensation results for the three absorbers as function of absorber thickness divided by scintillator thickness [Fig 3a] when the scintillator was held fixed at 0.25cm and as a function of scintillator thickness divided by absorber thickness [Fig 3b] when the absorber was held fixed at 0.25 radiation lengths. The two curves for each of the absorber materials represent calculations done with ESKALE set at 5 GeV, the lower curve, and set at 15 GeV, the upper curve. The gate width used in the calculations was 48 nsec. For the iron and lead cases this gate width is sufficient to collect the large majority of the signal. However for the uranium case this is not true due to the fact that uranium through fission processes produces additional neutrons and that uranium has a very large capture cross section at energies less than 1 MeV. In a large calorimeter system and in a high luminosity environment, the produced gammas may yield a significant contribution to background noise and thus produce pile-up problems. The experimental data points, even though they are from calorimeters not simulated by these calculations, are plotted to show that the calculations agree with the general trends. In addition the iron experimental data point represents a "weighted" value. The unweighted value is 1.36+/-0.04.

In Figure 3a we see that the iron calculations show that there seems to be no strong dependence of the compensation on absorber thickness. There is a stronger dependence for the lead and uranium cases. This is due, in part, to the strong Z dependence of the electromagnetic cross sections. In Figure 3b, the curves have to approach each other as the scintillator thickness becomes sufficiently large to contain both the electromagnetic and hadronic cascade.

In Figure 4a we present the hadronic resolution as a function of absorber thickness divided by the scintillator thickness which was held fixed at 0.25cm and in Figure 4b for scintillator thickness divided by absorber thickness which was held at 0.25 radiation lengths. Only the calculation done at an ESKALE 5 GeV is presented as the values for ESKALE at 15 GeV lie basically on top of the these values. The comparison with the uranium and

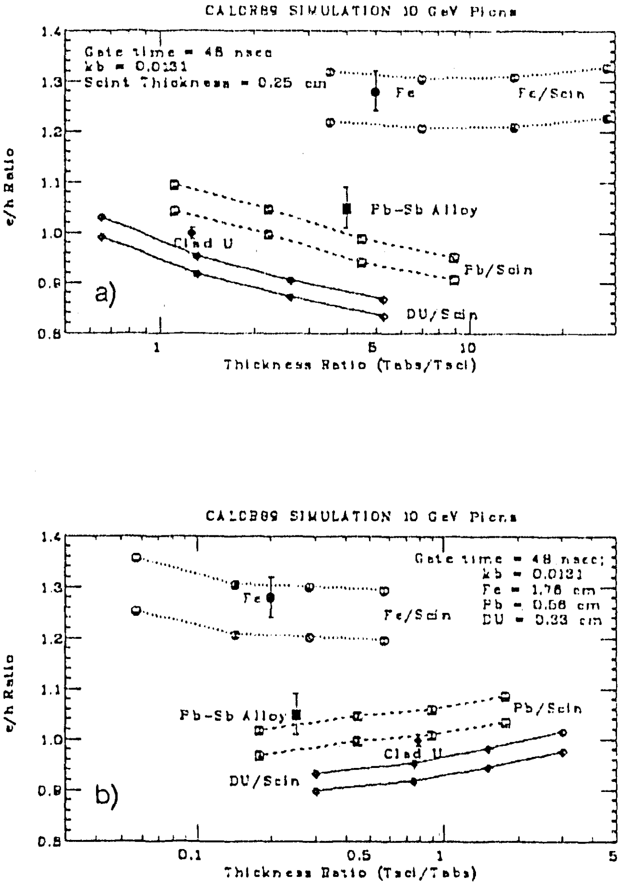

Figure 3. e/h is shown as a function of absorber thickness divided by a fixed scintillator thickness in 3a, while in 3b it is shown as a function of scinitllator thickness divided by a fixed thickness of absorber.

lead resolution data appears quite good. We feel that the disagreement between the iron calculation and the iron data point is probably due to the strong data cuts applied and to the lateral size of the calorimeter.

In Figure 5 we present similar curves for the electromagnetic resolution. The agreement between the calculations and the experimental data are again good except for the iron data point. As in the case of the hadronic data point we feel that their experimental cuts are possibly the cause.

It has been suggested that by placing hydrogenous material on either side of a plastic scintillator in conjuction with an iron absorber, that such a calorimeter could be made compensating. Calculations utilizing CALOR89 indicate at 10 GeV at most a 5% improvement in the compensation characteristics. The calculations that were carried out were for an iron absorber of thickness 2.54cm followed by 0.4cm hydrogenous material (dead scintillator) followed by 0.2cm of active scintillator followed by 0.4cm of hydrogenous material.

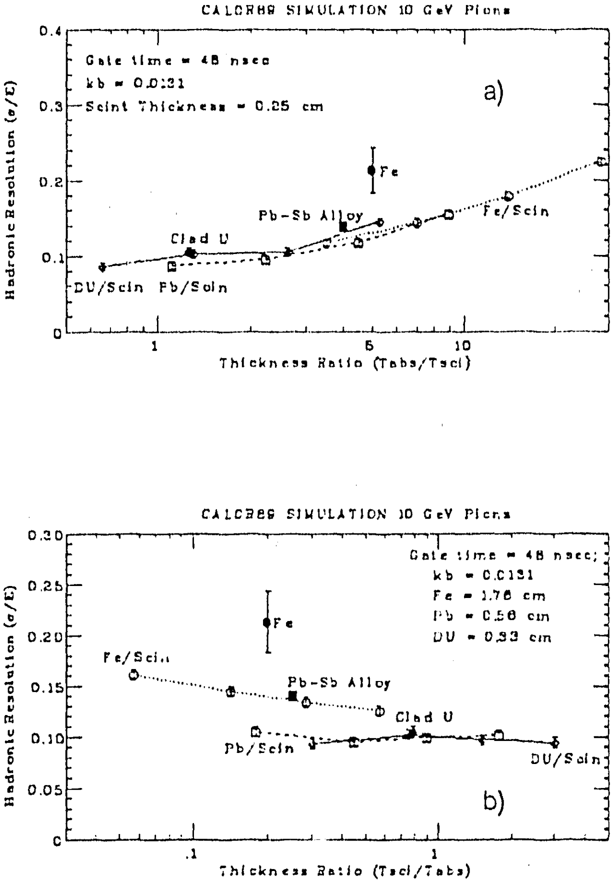

Figure 4. Hadronic resolution as a function of absorber divided by fixed scintillator in 4a and as a function of scintillator divided by fixed absorber in 4b.

This was repeated for 8 interaction lengths of iron.

Summary

The CALOR89 code system has been used to compare with various calorimeter prototypes. In general the agreement obtained has been satisfactory or discrepancies can be traced to experimental cuts, biases, leakage, etc. This code system has been used to generate preliminary design data for a variety of absorber, scintillator configurations. These results give general trends on the anticipated changes in the energy resolution and compensation characteristics.

References

[1] R. G. Alsmiller Jr., F. S. Alsmiller, and O. W. Hermann, "The High Energy Transport Code - HETC88 and Comparison with Experimental Data." Submitted to Nuclear Instruements and Methods.

[2] W. R. Nelson, et al., SLAC-265, Stanford Linear Accelerator Center, (1985).

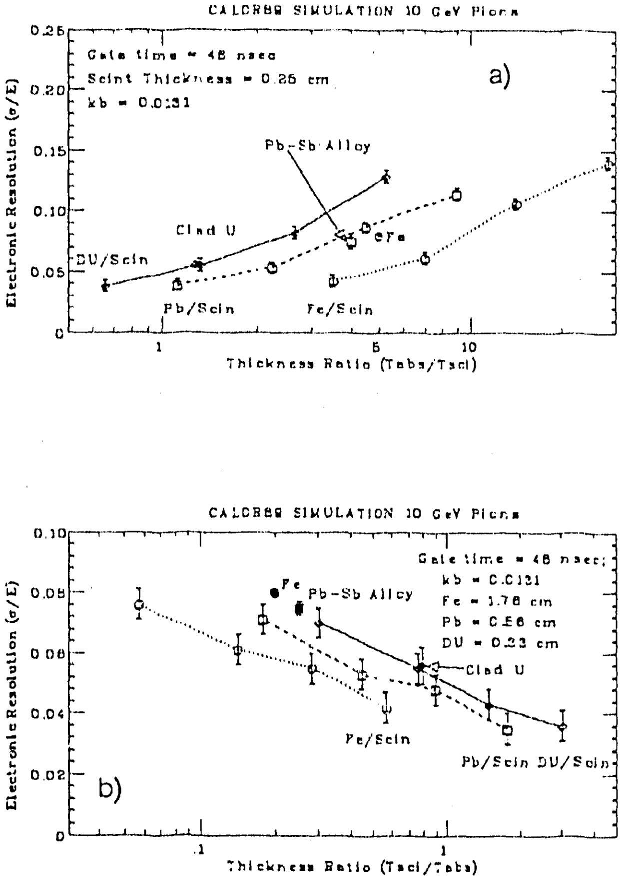

Figure 5. Electromagnetic resolution as a function of absorber divided by fixed scintillator in 5a and as a function of scintillator divided by fixed absorber in 5b.

[3] M. B. Emmett, ORNL-4972, Oak Ridge National Laboratory, (1975). N. M. Greene et al., ORNL/TM-3706, Oak Ridge National Laboratory, (1973).

[4] J. O. Johnson and T. A. Gabriel, ORNL/TM-10196, Oak Ridge National Laboratory, (1987).

[5] H. W. Bertini, Phys. Rev. 188(1969)1711.

[6] J. Ranft and S. Ritter, Z. Phys. C: Part. Fields 10(1981)249. P. A. Aarnio, et al., "CERN TIS Divisional Report, TIS-RP/106-Rev, 1984. A. Capella and J. Tran Thanh Van, Phys. Letts., 93B(1980)2.

[7] J. B. Birks, Proc. Phys. Soc., A64(1951)874.

[8] H. Abrahamowicz et al., Nucl. Inst. Meth., 180(1980)429.

[9] E. Bernadi et al., Nucl. Inst. Meth., A262(1987)229.

[10] E. Ros and T. Tsurugai, ZEUS Note 88-086(1988).

[11] M. Abolins, et al., Nucl. Inst. Meth., A280(1987)36.

END

DATE FILMED

01 / 09 / 91